AGU PUBLICATIONS

Earth and Space Science

RESEARCH ARTICLE
10.1002/2016EA000174

Key Points:
- Accumulated snowfall is a strong predictor of peak SWE and snow depth at SNOTEL and COOP sites
- For this data, spatial interpolation of SWE is improved by first normalizing by accumulated snowfall
- This interpolation produces maps of SWE comparable to existing maps that are based on much more data

Supporting Information:
- Supporting Information S1

Correspondence to:
P. D. Broxton,
broxtopd@email.arizona.edu

Citation:
Broxton, P. D., N. Dawson, and X. Zeng (2016), Linking snowfall and snow accumulation to generate spatial maps of SWE and snow depth, *Earth and Space Science*, *3*, 246–256, doi:10.1002/2016EA000174.

Received 22 MAR 2016
Accepted 26 MAR 2016
Accepted article online 7 APR 2016
Published online 9 JUN 2016

Linking snowfall and snow accumulation to generate spatial maps of SWE and snow depth

Patrick D. Broxton[1], Nicholas Dawson[1], and Xubin Zeng[1]

[1]Department of Atmospheric Sciences, University of Arizona, Tucson, Arizona, USA

Abstract It is critically important but challenging to estimate the amount of snow on the ground over large areas due to its strong spatial variability. Point snow data are used to generate or improve (i.e., blend with) gridded estimates of snow water equivalent (SWE) by using various forms of interpolation; however, the interpolation methodologies often overlook the physical mechanisms for the snow being there in the first place. Using data from the Snow Telemetry and Cooperative Observer networks in the western United States, we show that four methods for the spatial interpolation of peak of winter snow water equivalent (SWE) and snow depth based on distance and elevation can result in large errors. These errors are reduced substantially by our new method, i.e., the spatial interpolation of these quantities normalized by accumulated snowfall from the current or previous water years. Our method results in significant improvement in SWE estimates over interpolation techniques that do not consider snowfall, regardless of the number of stations used for the interpolation. Furthermore, it can be used along with gridded precipitation and temperature data to produce daily maps of SWE over the western United States that are comparable to existing estimates (which are based on the assimilation of much more data). Our results also show that not honoring the constraint between SWE and snowfall when blending in situ data with gridded data can lead to the development and propagation of unrealistic errors.

1. Introduction

Runoff production in cold regions is heavily influenced by snowmelt, and in some regions, such as the semiarid western Conterminous United States (ConUS), snowmelt is the most important contribution to water resources [e.g., *Bowling et al*., 2003; *Bales et al*., 2006]. In these regions, it is particularly important to quantify the amount of snow on the ground. For example, in the western ConUS, water supply forecasts are heavily reliant on correlations between river flows and snow water equivalent (SWE) measurements at Snow Telemetry (SNOTEL) stations [*Serreze et al*., 1999]. These correlations are useful, but gridded estimates of SWE or snow depth are preferable for a variety of purposes including water balance studies or model evaluation.

There is much uncertainty about using point measurements to improve gridded estimates of SWE or snow depth because of differences in horizontal scale and uncertainties about the representativeness of the measurements. For example, snow data at SNOTEL stations can be unrepresentative of surrounding areas [e.g., *Molotch and Bales*, 2006] because they are typically located at higher elevations and in areas that accumulate deeper snowpacks than a majority of the area surrounding them. At the same time, other data sets (e.g., the National Weather Service Cooperative Observer (COOP) data) are biased toward lower elevations because they are typically collected in or near population centers [*Brasnett*, 1999] and so may underrepresent the amount of snow in a given region.

Elevation, distance from a given station, and/or other factors related to topography, vegetation, or radiation are commonly used to upscale point measurements of SWE over areas [e.g., *Brasnett*, 1999; *Brown et al*., 2003; *López-Moreno and Nogués-Bravo*, 2006; *Fassnacht et al*., 2003; *Erxleben et al*., 2002]. However, at larger scales (tens to hundreds of kilometers), these factors do not always predict trends in SWE. For example, the windward sides of mountain ranges commonly receive more precipitation than the leeward sides [e.g., *Daly et al*., 1994]. Because the amount of SWE on the ground is highly dependent on the amount of snow that fell [*Blanchet et al*., 2009; *Schirmer et al*., 2011], a well-constrained estimate of snowfall is likely a better predictor of snow on the ground, especially as it is the physical reason for the snow being there in the first place.

One way to incorporate information about precipitation while "interpolating" point measurements is to combine them with model estimates of SWE, as is done for the National Operational Hydrologic Remote Sensing Center's (NOHRSC) Snow Data Assimilation System (SNODAS) [*Carroll et al*., 2001] as well as for

various short- and medium-range weather forecasting models (e.g., at the Canadian Meteorological Center (CMC) [*Brown and Brasnett*, 2010] and the European Centre for Medium-Range Weather Forecasts (ECMWF) [*Drusch et al*., 2004] and by various investigators [e.g., *Raleigh and Lundquist*, 2012; *Guan et al*., 2013]. Precipitation is accounted for in this combination of observations and model estimates because it is one of the variables used to force the snow model.

However, the *methodologies* to blend observed and modeled SWE do not generally account for differences in snowfall between points and grid boxes. For example, the interpolation method used at the CMC's daily snow depth analysis for the entire Northern Hemisphere, which is widely used for land model evaluations [e.g., *Niu and Yang*, 2007; *Reichle et al*., 2011], relies on correlation functions of distance and elevation to relate grid box SWE to point data, regardless of differences in the snowfall that occurred. SNODAS is nudged toward snow observations using a Newtonian Relaxation Procedure if it is determined by an analyst that such nudging is necessary [*Barrett*, 2003], though we are unable to obtain full details about this procedure in peer-reviewed literature. Such interpolation and nudging do not honor the physical processes for snow being on the ground in the first place and hence may result in mismatches between SWE and the precipitation that produced the SWE.

In this study, we first compare how well the spatial patterns of SWE or snow depth at peak snow accumulation at SNOTEL and COOP stations can be predicted using our new interpolation technique based on the relationship between accumulated snowfall and SWE (or snow depth) versus four other interpolation methods that do not consider differences in snowfall. Next, we demonstrate the use of our new technique to produce daily gridded SWE estimates with high-quality gridded precipitation and temperature data from the Parameter Regression on Independent Slopes Model (PRISM) [*Daly et al*., 1994] at 2.5 arc min resolution. We place more of an emphasis on SWE than snow depth because SWE is the variable that is of most interest hydrologically (e.g., for determining how much potential melt there can be).

2. Data and Methods

2.1. Observational Data

This study uses observations of SWE, snow depth, and precipitation at SNOTEL stations and observations of snow depth and precipitation at COOP stations. SNOTEL stations are typically located at higher elevations in remote mountainous sites. As such, they receive much more snowfall than COOP stations. For example, of the 555 SNOTEL and 473 COOP stations used in this study (see below), the 5th–95th percentiles of snowfall at the SNOTEL sites ranged from 234 mm to 1557 mm, while at the COOP sites, they ranged from 11 mm to 364 mm during Water Year (WY) 2008. Due to the remote location of many of the SNOTEL stations, measurements are automatic. For COOP stations, measurements of snow depth and precipitation are manual, and there is typically no measurement of SWE.

To generate spatial maps of SWE (described below in section 2.3 and presented in section 3.4), this study also uses daily gridded precipitation and temperature data from PRISM. PRISM generates gridded estimates of precipitation and temperature using statistical relationships and coordinated rules to produce spatial maps of precipitation and temperature [*Daly et al*., 1994, 2008]. It incorporates data from 13,000 stations for precipitation and nearly 10,000 stations for maximum and minimum temperature across the ConUS [*Daly et al*., 2008]. The basis for PRISM is a climate-elevation regression that varies spatially, but it also accounts for a variety of local factors affecting climate, such as rain shadow affects, temperature inversions, and the effects of nearby water bodies on temperature and precipitation. PRISM is especially well suited for interpolating climate data in physiographically complex landscapes [*Daly et al*., 2008].

SNOTEL and COOP sites are only retained if they have a snow accumulation period that lasts longer than 1 day and if there is no missing precipitation data during the snow accumulation period. In addition, we manually inspected all time series for all sites to remove obvious spurious data, mainly affecting the snow depth data. This results in a limited number of stations being retained for analysis. For example, after all quality checks, 555 SNOTEL and 473 COOP stations (out of 622 and 12472 stations, respectively) are retained across the western ConUS for WY 2008. These locations are shown in Figure 1. We do not apply quality control to the PRISM data as there is already extensive quality control of the station data that is used in PRISM [*Daly et al*., 2008].

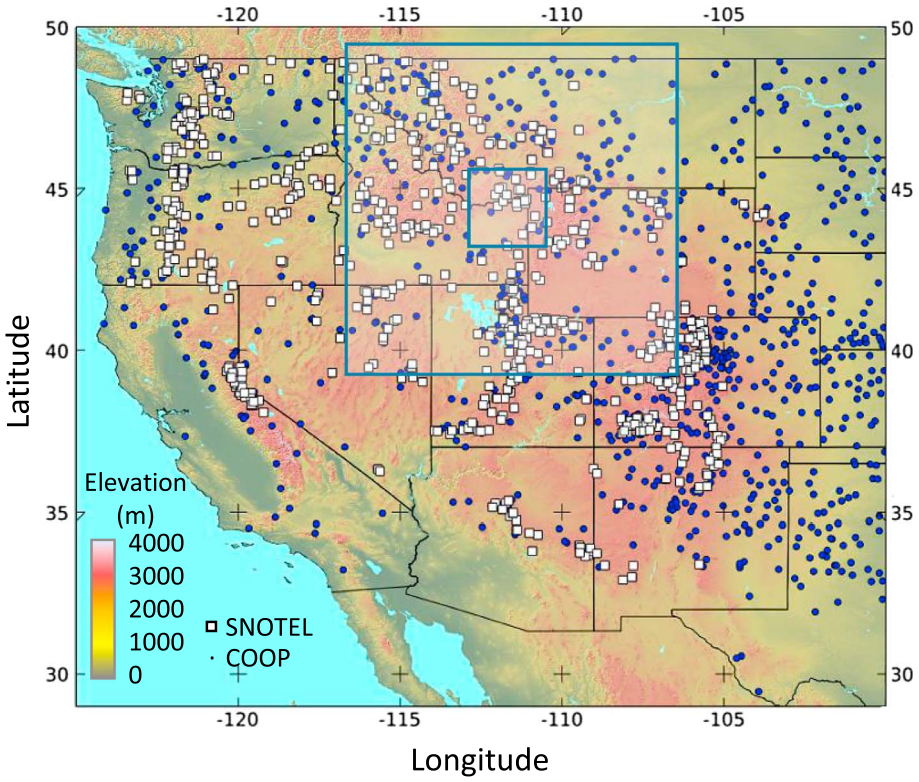

Figure 1. Locations and elevations of COOP and SNOTEL stations that are used in this study. Also shown are the 2° × 2° and 10° × 10° grid boxes used for the analysis in sections 3.2.

Following *Knowles et al*. [2006] and *Huntington et al*. [2004] who performed studies of trends in snowfall in the western and eastern U.S., respectively, we compute snowfall at COOP stations as the precipitation totals on days for which there was newly fallen snow. Similarly, at SNOTEL stations, it is computed as the precipitation totals on days when there is a positive change in SWE. In general, *Knowles et al*. [2006] and *Huntington et al*. [2004] show that this method partitions between rainfall and snowfall reasonably well in both the western and eastern ConUS. We partition daily PRISM precipitation data into rainfall and snowfall using a daily temperature threshold. The determination of this threshold and accounting for its uncertainty is discussed in section 2.3 below.

2.2. Method for the Cross Validation of SWE_{max} and D_{max} Predictions at SNOTEL and COOP Stations

To quantify the degree to which including information about accumulated snowfall can improve spatial estimates of SWE and snow depth, we perform a cross-validation experiment where we compare how many SNOTEL stations are needed to predict SWE at "unknown" stations for two different scales using snowfall as a constraint versus only using distance and elevation. Our analysis focuses on a 2° × 2° box and a 10° × 10° box (having areas of approximately 150 km × 220 km and 750 km × 1100 km) in the Northern Rockies. We focus on peak of winter SWE (SWE_{max}) and peak of winter snow depth (D_{max}) as these quantities capture the integrated effects of snowfall and ablation that occurs prior to the date of SWE_{max} and D_{max}.

To establish a baseline, this study uses four previous methods to estimate D_{max} and SWE_{max} at the unknown stations: inverse distance weighting of SWE measurements (referred to as *idw*), inverse distance weighting of residuals of a hypsometric relationship (between SWE_{max} or D_{max} and elevation; referred to as *idw+h*), ordinary Kriging of residuals of this hypsometric relationship (referred to as *krig+h*), and optimal interpolation (OI) [*Brasnett*, 1999], a method for the interpolation of residuals from a background field of SWE, accounting for both horizontal and vertical distances. The OI method is currently used to combine modeled snow depths with those measured at stations at both the CMC and ECMWF, so it can be considered as the state of the art. To maintain consistency with *idw+h* and *krig+h*, the background is determined from the regression

between SWE_{max} (or D_{max}) with elevation (referred to as *OI+h*). These methods are well known and have been previously published [e.g., *Brasnett*, 1999; *Erxleben et al*., 2002; *Fassnacht et al*., 2003], but for convenience, the mathematical details of these methods are provided in the supporting information.

Estimates of SWE_{max} (or D_{max}) at unknown stations using these methods are then compared to estimates of SWE_{max} (or D_{max}), using our new method: the interpolation of SWE_{max} (or D_{max}), normalized by accumulated snowfall (in this study, "accumulated snowfall" refers to the snowfall that occurs from the last snow-free date up until the time of peak of winter snow accumulation). Here we test two situations: (1) when SWE_{max} or D_{max} at unknown stations is predicted with SWE_{max} or D_{max} at known stations as well as accumulated snowfall for the current year and (2) when SWE_{max} or D_{max} at unknown stations is predicted with SWE_{max} or D_{max} at known stations as well as a climatology of accumulated snowfall. For our first method (called *krig+S*), SWE_{max} (or D_{max}) divided by accumulated snowfall is computed at each known station; these values are interpolated to the unknown stations using ordinary Kriging, and these interpolated values are multiplied by accumulated snowfall at those unknown stations to compute SWE_{max} or D_{max}. For our second method (called *krig+cS*), SWE_{max} (or D_{max}) divided by the climatological average of accumulated snowfall is computed at each known station; these values are interpolated to the unknown stations, and the interpolated values are multiplied by the climatological average of accumulated snowfall at those unknown stations to compute SWE_{max} or D_{max}.

In this study, the period of climatology was WY 2005–2007. We used this short climatology period because increasing the number of years would increase the number of stations with missing data (which was especially an issue for the COOP data). In addition, we found that we only needed a few years to adequately determine climatological differences between different locations. For example, the coefficient of determination (R^2) between SWE_{max} for all SNOTEL stations for 2008 and the average SWE_{max} for the period 2005–2007 is 0.66. The R^2 only increases to 0.71 if the average SWE_{max} for the period 1980–2007 is compared to the SWE_{max} in 2008.

For each interpolation methodology, we performed a *leave-p out* cross validation whereby we used *p* stations to generate predictions at the remaining stations. The number of predictor stations, *p*, ranges from five stations to the number of stations available minus 1. For each value of *p*, the predictor stations are also chosen randomly 100 times to assess the error in the predictions at the remaining stations.

We only analyzed stations with data that meets the standards outlined in section 2.1 for all years of the climatological period (2005–2007; as all of these data are used by our *krig+cS* method). This especially limits the number of COOP stations that can be used because of the large amount of missing data at the COOP stations. For the $10° \times 10°$ grid box, 214 SNOTEL and 27 COOP stations are used in these analyses. For the $2° \times 2°$ grid box, only 15 SNOTEL stations are used.

2.3. Method for Creating Gridded Estimates of SWE From SNOTEL Measurements

We then use our *krig+S* interpolation method to generate gridded estimates of SWE using PRISM precipitation and temperature data and SNOTEL SWE data for the $10° \times 10°$ box. We compute these SWE estimates on the same grid as the original PRISM data, which has a 2.5 arc min resolution (approximately 2.6×3.75 km per grid cell for our study domain) and a daily time step. Here SWE is divided by net accumulated snowfall, defined as accumulated snowfall (measured at the SNOTEL stations) minus an estimate of cumulative ablation (from the first date that snow is covering the ground to the analysis date). We include ablation here because after peak SWE at higher elevations (as well as throughout the winter at lower elevations), the amount of snow on the ground depends significantly on how much ablation occurs in addition to the amount of snowfall that occurs, whereas above, we only consider peak SWE at SNOTEL stations, which is predicted well by accumulated snowfall alone (see section 3.1 below). Then, as above, we interpolate (Krig) these values of SWE divided by net accumulated snowfall to each grid cell in the $10° \times 10°$ box and multiply the interpolated values by net accumulated snowfall to find the resulting SWE estimates at each grid cell. For these tests, we only use the 214 (all available) SNOTEL stations in the $10° \times 10°$ box because the COOP stations do not record SWE.

The rules governing net accumulated snowfall (both accumulated snowfall and cumulative ablation) are based on SNOTEL data. We consider precipitation to be rain or snow based on whether the mean daily temperature is greater or less than +2°C. This threshold appears to be reasonable in the $10° \times 10°$ box because the fraction of days with precipitation at the SNOTEL stations that results in an increase in SWE is about half (48%)

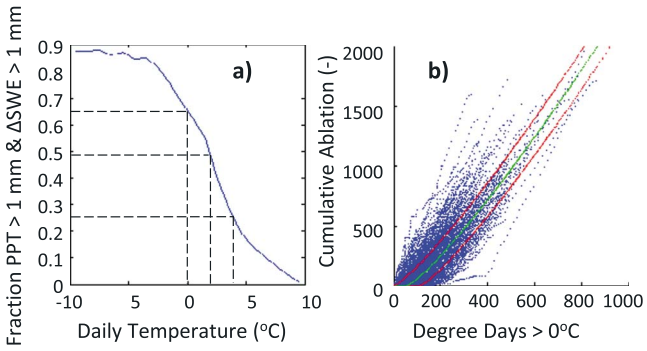

Figure 2. (a) Shows, in 1°C daily temperature increments, the fraction of wet days (when precipitation >1 mm) that are associated with an increase in SWE at SNOTEL stations. The horizontal and vertical black lines show the temperatures corresponding with values of 0.25, 0.48, and 0.65 (fractions of wet days) referred to in section 2.3. (b) The cumulative ablation (represented as accumulated snowfall minus SWE) plotted against the number of degree days above 0°C based on all the SNOTEL data in the 10° × 10° grid box in Figure 1. Each blue dot represents a daily measurement of accumulated snowfall minus SWE. The green line shows a best fit regression for the data. The red lines show this function shifted by equal distances in the positive and negative *x* direction such that the area between the curves captures 75% of the data points.

at +2°C (Figure 2a). Then, as above, we compute accumulated snowfall as the sum of these daily snowfalls while there is continuous snow cover. Cumulative ablation is taken to be a function of cumulative degree days above 0°C during the snow-covered period. This relationship is given by the difference between accumulated snowfall and SWE versus cumulative degree days above 0°C at the SNOTEL stations. This relationship is shown by the green line in Figure 2b, which is a best fit regression of all the cumulative ablation versus cumulative degree day data pairs across the entire network for the entire snow season. These rules are then applied to both the SNOTEL and PRISM precipitation and temperature data to estimate net accumulated snowfall for each day at each station and each grid cell.

Given that there is considerable uncertainty in the relationships shown in Figures 2a and 2b, we perform a "low snow" simulation and a "high snow" simulation to get a sense of uncertainty. For the low snow simulation, the temperature threshold that defines whether precipitation on a given day is considered as rain or snow is set to 0°C (resulting in less snowfall), and for the high snow simulation, it is set to +4°C (resulting in more snowfall). Note that at 0°C, the SNOTEL data suggest that 65% of days with precipitation have an associated increase in SWE, and at +4°C, 25% of days with precipitation have an associated increase in SWE (Figure 2a). In addition, for the low snow simulation, cumulative ablation is modeled by the leftmost red line in Figure 2b (resulting in more ablation at low temperatures), and for the high snow simulation, it is modeled by the rightmost red line in Figure 2b (resulting in less ablation). Seventy-five percent of the data points lie within the red lines in Figure 2b.

We then compare the resulting SWE maps with those from the National Operational Remote Sensing Center (NOHRSC)'s Snow Data Assimilation System (SNODAS) [*Carroll et al*., 2001] product that assimilates snow information from ground-based, airborne, and satellite platforms. While SNODAS is not the ground truth, it still provides a useful benchmark for our comparison because of its wide use. The 30 arc sec SNODAS product is resized to 2.5 arc min resolution using bilinear interpolation to match the resolution of the PRISM (and our gridded SWE) data.

3. Results

3.1. The Spatial Consistency of SWE_{max} and D_{max} When Normalized by Snowfall

The SNOTEL and COOP data show substantial spatial variability of SWE_{max} and D_{max} (Figures 3a and 3b). Considering all SNOTEL sites in the western ConUS, the interquatile range (i.e., the difference between the 75th and 25th percentiles; denoted as Q75-Q25) of SWE_{max} during the water year (WY) 2008 was 406 mm (Figure 3a), and the Q75-Q25 of D_{max} values recorded at COOP sites during WY 2008 was 457 mm (Figure 3b). This spatial variability makes it challenging to do the spatial interpolation using techniques presented in previous publications (to be demonstrated in section 3.2).

At the same time, accumulated snowfall is a relatively strong predictor of SWE_{max} and D_{max}. For example, the Q75-Q25 of the residuals on the regression of accumulated snowfall with SWE_{max} and D_{max} shown in Figures 3c and 3d are just 99 mm and 122 mm, respectively. Furthermore, normalizing SWE_{max} and D_{max} by the regressions in shown in Figures 3c and 3d reduces the spatial variability shown in Figures 3a and 3b. For example, the 75th percentile divided by the 25th percentile (denoted Q75/Q25) of SWE_{max} values

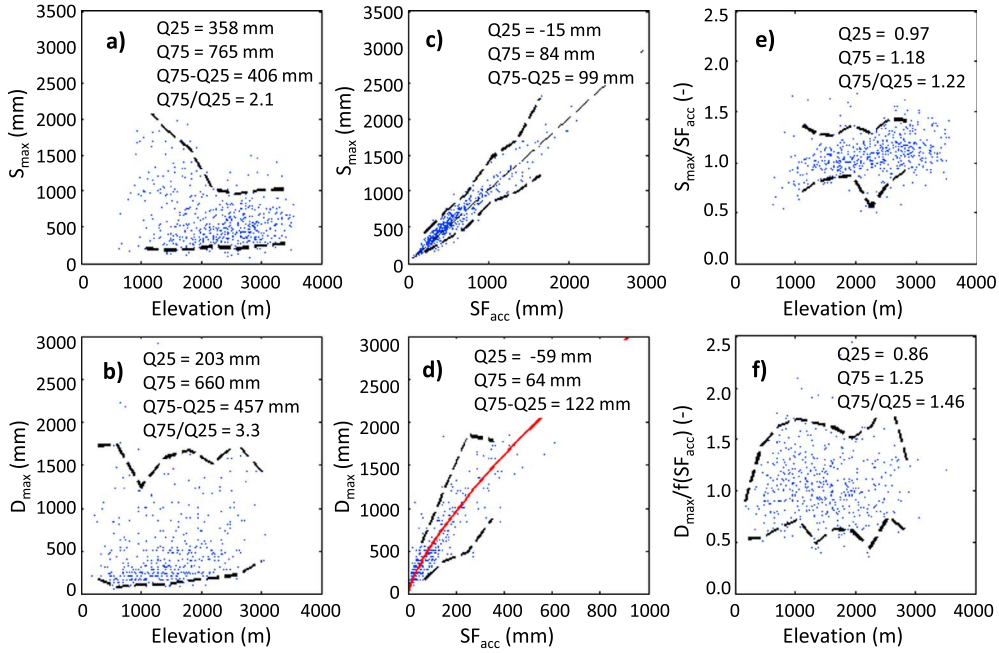

Figure 3. Scatterplots of WY 2008 values for all SNOTEL stations of (a) SWE_{max} versus elevation, (c) SWE_{max} versus accumulated snowfall (SF_{acc}), and (e) SWE_{max}/SF_{acc} versus elevation. The results for all COOP stations are shown in (b) D_{max} versus elevation, (d) D_{max} versus SF_{acc}, and (f) $D_{max}/f(SF_{acc})$ (where $f(SF_{acc})$ is the regression shown by the thick red line in Figure 3d for all COOP stations). Figure 3c also shows the regression between SWE_{max} versus SF_{acc} for all SNOTEL stations (thin black dashed line). The thick black dashed lines in all panels show the 5th and 95th percentiles of the data (to be consistent with subsequent figures) for each bin in abscissa. In Figures 3a, 3b, 3e, and 3f, the text shows the 25th and 75th percentiles of the data set as a whole, while the 25th and 75th percentiles of the residuals on the regression between SF_{acc} and SWE_{max}/D_{max} are shown in Figures 3c and 3d.

recorded at SNOTEL stations reduces from 2.1 (Figure 3a) to 1.2 when the values are divided by accumulated snowfall (Figure 3e), and the Q75/Q25 of D_{max} values recorded at COOP sites reduces from 3.3 (Figure 3b) to 1.5 (Figure 3f) when divided by the regression equation shown in Figure 3d.

This substantial reduction in scatter implies that it is easier to obtain spatially consistent estimates of the normalized quantities (to be demonstrated in sections 3.2 and 3.3), despite the uncertainties in the data (e.g., gauge undercatch of snowfall). One note of caution is that SNOTEL and especially COOP measurements are probably mostly located in ideal flat settings. *Grünewald and Lehning* [2015] found that ideal, flat measurements tend to overestimate SWE and snow depth for close surroundings (up to 400 m horizontal distance), though *Helbig et al.* [2015] found that there is much better agreement between flat measurements and spatially averaged snow depth for larger grid cells (>1500 m), such as those used in this study.

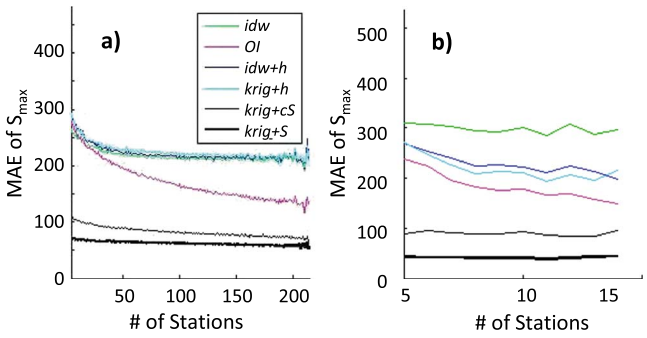

Figure 4. (a) The mean absolute error (in mm) between measured and predicted values of SWE_{max} at unknown SNOTEL stations (those where SWE_{max} are predicted from other stations) using the four previous methods and our two new methods (*krig+cS* and *krig+S*), as a function of the number of stations used to do the prediction within the 10° × 10° grid box in Figure 1. (b) The corresponding results for the 2° × 2° grid box.

3.2. Predicting Peak SWE at SNOTEL Sites Using Multiple Interpolation Techniques

Fewer stations are needed to produce more accurate estimates of SWE_{max}

Table 1. Error of Predictions of SWE_{max} and D_{max} Compared to Observations[a]

	SNOTEL	COOP
	SWE_{max}	D_{max}
idw	217.8	373.1
b99	170.1	412.0
idw+h	222.1	387.9
krig+h	225.2	386.1
krig+cS	82.3	200.5
krig+S	61.9	185.6

[a]Column 1 shows the average MAE (in mm) between observed and predicted SWE_{max} at the 214 SNOTEL stations in the 10° × 10° box for the four previous methods (*idw*, *OI*, *idw+h*, and *krig+h*) and our two new methods (*krig+S* and *krig+cS*). Column 2 shows the same quantities but for predictions of D_{max} at 27 COOP stations in the 10° × 10° box.

given knowledge of accumulated snowfall (i.e., *krig+S*), both at the larger scale (10° × 10° box) and at the smaller scale (2° × 2° box) as compared with the four previous methodologies that do not use accumulated snowfall (Figure 4 and column 1 of Table 1). At both scales, the mean absolute error (MAE), computed as the average of the absolute differences between observed values and those predicted by each of the six interpolation methodologies at *unknown* stations, is generally close to 10% of the average SWE_{max} for our method (*krig+S*), while for the previous methods, it is generally 25–40% of the average SWE_{max} (though OI clearly performs better than the other three methods). At the larger scales, using 22 stations to predict SWE_{max} at the remaining stations, the average of MAE (232 mm) using the four previous methods is 4.8 times as large as that using our method, and this ratio remains as large as 2.9 even when 200 stations are used as predictors (Figure 4a). At the smaller scale, the ratio is even larger (e.g., 6.6 with 5 stations used as predictors and 6.0 with 14 stations used as predictors) (Figure 4b). In short, at the scales that we examine, accumulated snowfall helps predict SWE_{max} at unknown stations far better than elevation does.

Although information about accumulated snowfall for the current water year at unknown sites is best, climatological knowledge of accumulated snowfall can still be used to produce relatively accurate estimates of SWE_{max}. Fox example, the MAE of predictions versus measurements of SWE_{max} at unknown stations using our *krig+cS* method is generally less than half of those estimated using the four previous methods (Figure 4 and column 1 of Table 1). Additional tests indicate that for SNOTEL stations, SWE_{max} can also be predicted almost equally as well by climatological values of SWE_{max} as by climatological values of accumulated snowfall. This is unsurprising given the recognized interannual consistency of patterns of SWE [e.g., *Deems et al*., 2008; *Schirmer et al*., 2011].

3.3. Linking SNOTEL and COOP Measurements of Peak Snow Depth

Accumulated snowfall can also be used to link the SNOTEL and COOP data sets, which, as noted in section 2.1, receive quite different amounts of snowfall. Therefore, COOP stations can be used as an independent test of the robustness of the results obtained for SNOTEL stations. We perform exactly the same analysis on the COOP data, with the only difference being that D_{max} is normalized by the regression between D_{max} and accumulated snowfall shown in Figure 3d instead of accumulated snowfall itself. This is because the regression between D_{max} and accumulated snowfall is slightly nonlinear (Figure 3d), which is largely a reflection of the nonlinear relationship between snow depth and SWE (i.e., snow depth does not increase linearly with SWE).

The differences between SNOTEL and COOP sites can be seen for the 10° × 10° box in Figure 1 by comparing the two columns of Table 1. In both cases (predicting SWE_{max} at SNOTEL sites or D_{max} at COOP sites), both of our *krig+S* and *krig+cS* methods perform best: for the SNOTEL SWE_{max} predictions, the MAE for unknown stations for *krig+cS* is 133% of that computed for the *krig+S* method, while for the four previous methods, this MAE ranges from 275 to 364% of that computed for the *krig+S* method. For the COOP D_{max} predictions, the MAE for unknown stations for *krig+cS* is 108% of that computed for the *krig+S* method, while for the four previous methods, this MAE ranges from 201 to 222% of those computed for the *krig+S* method.

Accumulated snowfall is also useful for predicting peak of winter snow accumulation outside the range of climatic conditions that are represented in each individual data set. For example, *krig+S* and *krig+cS* can better predict COOP D_{max} using SNOTEL D_{max} data or predict SNOTEL D_{max} using COOP D_{max} data compared with the four previous methods. Figure 5 shows that using the same methodology as above (except that the entire COOP data set is used to estimate the entire SNOTEL data set in the larger grid box, and vice versa),

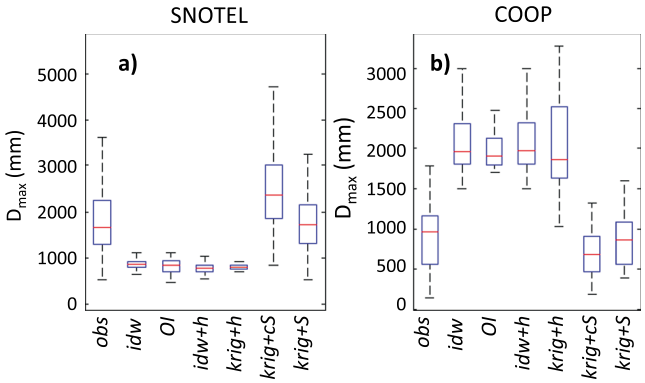

Figure 5. Box plots showing the observed (obs) and predicted D_{max} using four previous methods (*idw*, *OI*, *idw+h*, and *krig+h*) and two new methods (*krig+cS* and *krig+S*) at (a) SNOTEL stations (using all COOP data only for regression in these methods) and (b) COOP stations (using all SNOTEL data only for regression in these methods) in the 10° × 10° grid box in Figure 1.

krig+S and *krig+cS* predict both a much more realistic median D_{max} and a much smaller MAE between observed and predicted D_{max} than the four previous methods. This is despite the fact that the SNOTEL stations (typically located in mountainous locations) have higher D_{max} than the COOP stations (typically located in population centers, commonly away from the mountains). In each case, the *krig+S* method performs the best, followed by *krig+cS*. The four previous methods severely overestimate the COOP D_{max} (Figure 5b) and underestimate the SNOTEL D_{max} (Figure 5a).

3.4. Application to Gridded Data

In general, our *krig+S* method (using only information from PRISM and SNOTEL data and normalizing SWE by net accumulated snowfall) generates SWE maps that are comparable to the SNODAS product, even though it assimilates much less SWE data. This can be seen by comparing the peak of winter snow accumulation in the SNODAS product versus using our *krig+S* method (Figure 6f and comparing Figure 6a with Figure 6b) with R^2 between these maps being 0.79 and the mean absolute difference between the maps being 70 mm (or 35% of the average SWE in the SNODAS map). At high elevations, the differences between our map and the SNODAS map are generally less than 20% of the SWE_{max} value.

This level of agreement between the SWE maps generated using our *krig+S* method and the SNODAS maps lasts for much of the winter. In fact, from the time that significant snow accumulation begins in mid-November to the time of peak of winter snow accumulation in late March and April, R^2 between the two maps is generally about 0.8 (blue solid line in Figure 6l), and the mean absolute difference is less than one third of the average SWE value (compare the blue solid lines in Figures 6j and 6k). Even though the high snow (or low snow) simulation predicts generally more (or less) SWE than is suggested by the SNODAS data, the R^2 between these simulations and the SNODAS map remains high through the winter, and the mean absolute difference remains low (blue dotted lines in Figures 6j–6l).

For comparison, we also implemented the best performing of the previous methods (*OI+H*) as well at the same resolution. Compared with *krig+S*, *OI+H* generally results in more snow at lower elevations, though the high elevations are predicted fairly well (compare Figures 6b and 6c with Figure 2a, and compare Figure 6f with Figure 6g). Overall, the resulting spatial R^2 of *OI+H* (with the SNODAS product) is similar to that of *krig+S* (light blue line in Figure 6l), though *OI+H* also has a much higher mean absolute difference with the SNODAS map than *krig+S* (Figure 6k). Furthermore, *OI+H* generally overestimates SWE compared to SNODAS or *krig+S*, and the estimated SWE, at times, even exceeds accumulated snowfall, which is unrealistic (Figure 6j). In contrast, the SWE estimates generated with *krig+S* increases fairly closely with accumulated snowfall for the early part of the winter, consistent with the SNODAS estimates.

We also implemented the optimal interpolation (OI) method using several other methods to obtain first guess fields. For the first case (referred to as *OI* (*cyc*) in Figure 6), it is implemented similar to *Brasnett* [1999], where the previous day's SWE, plus daily snowfall minus daily ablation, is used as an initial first guess for each day. Second, it is implemented using net accumulated snowfall as a first guess field for each day (referred to as *OI+S* in Figure 6). The difference is that for the first case, any alterations that were made during the previous day due to interpolation are preserved and carry through to subsequent days. For the second case, the effects of any interpolation do not carry over from day to day. The first case is analogous to how it is used to assimilate snow data for various data assimilation systems, and the second case makes its implementation very similar to *krig+S* (except when OI is used to distribute the residuals instead of Kriging). For the first case, estimated SWE diverges substantially from the SNODAS data, and this divergence gets worse

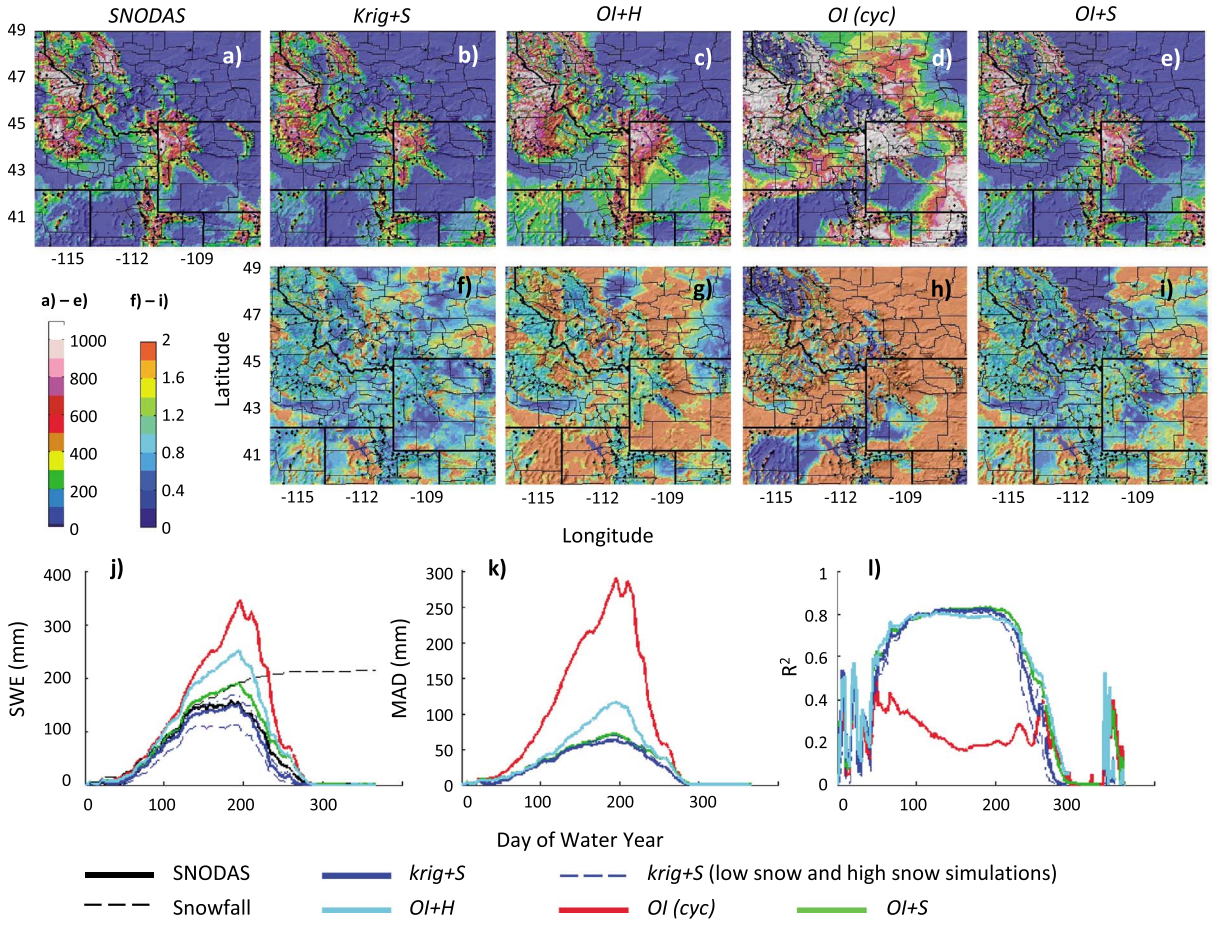

Figure 6. (a–e) Spatial maps of peak of winter SWE (computed, for each pixel, as the maximum of the daily SWE maps during WY 2008 for the 10° × 10° grid box for the SNODAS data), for *krig+S* (modified to use net accumulated snowfall in the normalization) and for optimal interpolation using just elevation information as above (*OI+H*), using the previous interpolated SWE value as a first guess [*OI* (*cyc*)], and using net accumulated snowfall as a first guess (*OI+S*). (f–i) The ratio of the maps in Figures 6b–6e to the map in Figure 6a. (j) The spatial average SWE in the 10° × 10° grid box through the course of the snow season for all data shown in Figures 6a–6e as well as the area-averaged accumulated snowfall on each day (monotonically increasing dashed black line). (k) The seasonal evolution of the mean absolute difference (MAD) between *krig−S*, *OI+H*, *OI* (*cyc*), and *OI+S* versus the SNODAS data. (l) The seasonal evolution of the R^2 value between *krig−S*, *OI+H*, *OI* (*cyc*), and *OI+S* versus the SNODAS data.

through the course of the winter (red lines in Figures 6j–6l) as the effects of the interpolation (whose spatial patterns are inconsistent with those of snowfall) add up from day to day. Basically, it results in far too much snow being added to many areas (as well as not enough snow being added to others; Figures 6d and 6h). On average, these SWE estimates significantly exceed accumulated snowfall through the winter. For the second case, results are much closer to the SNODAS data and the results from the *krig+S* method (green lines in Figures 6j–6l). There is no divergence because the effects of the previous days' interpolation do not carry over from day to day. Overall, there is slightly more SWE than the *krig+S* method predicts, and there is slightly larger disagreement with the SNODAS data.

4. Discussion and Summary

This study demonstrates that there is a strong link of accumulated snowfall, with SWE_{max} and D_{max} at SNOTEL and COOP stations that is valuable for estimating SWE over large areas up until the time of peak of winter snow accumulation (as shown by the strong correlations between snowfall and SWE_{max} in Figure 3c). We recognize that the strength of this linkage at SNOTEL locations is largely due to the fact that they are located high in the mountains where there is not a lot of midwinter melt. At lower elevations, where there is a lot of midwinter melt (e.g., at the COOP stations), this linkage only applies for short periods between snowfall

events and the maxima of snow accumulation that occurs immediately following one or a number of snowfall events. Another potential limitation is that even though the SNOTEL and COOP data, taken together, represent both high-SWE (SNOTEL) and low-SWE (COOP) environments, there are still many areas that are not characterized by these data sets. For example, across the western ConUS, there are not many COOP stations at higher elevations in areas where there are no SNOTEL stations.

We have shown that fewer "known" SNOTEL and COOP stations are required to represent SWE_{max} and D_{max} at unknown stations given knowledge of accumulated snowfall from the current or previous water years over interpolation that is based on distance and elevation only (Figure 4). Among the four previous interpolation methods based on distance and elevation, optimal interpolation (OI) can generate the most realistic estimates of SWE at validation points, likely because this method combines horizontal and vertical correlation distances to adjust snow quantities. This linkage has implications for applications that involve upscaling from point measurements to grid boxes (e.g., for gridded snow data estimation) and downscaling from grid boxes to point measurements (e.g., for model evaluation). SWE_{max} and D_{max} are much more spatially consistent, when normalized by accumulated snowfall (Figure 3), suggesting that the normalized quantities are more scale independent than unnormalized quantities.

This method, modified to include a representation of snow ablation, is applied to produce gridded PRISM-based estimates of snow data. Our method, using relatively simple interpolation of SWE normalized by net snowfall with a limited number of stations, can produce gridded estimates of SWE which are consistent with the widely used SNODAS estimates of SWE (which uses more complicated energy balance snow modeling and much more information in the data assimilation) over large areas in the western ConUS. Our method also ensures that the gridded representation of SWE remains consistent with the gridded representation of precipitation and ablation. The results shown in section 3.4 (allowing the interpolated residuals from previous days influence the current day's background field versus constructing the current day's background field from net snowfall) demonstrate that not honoring this constraint can result in unrealistic mismatches between spatial patterns of precipitation and spatial snow variability.

It could be argued that the use of precipitation data in snow analysis is not new, as gridded precipitation and other near-surface atmospheric data (solar and longwave radiation, temperature, wind, and humidity) are widely used in land models to produce gridded SWE and snow depth data through the assimilation of surface, airborne, and satellite measurements [e.g., *Rodell et al*., 2004]. Such gridded snow products are also available through data assimilation from global analysis [e.g., *Saha et al*., 2014] and reanalysis [e.g., *Rienecker et al*., 2011]. Our evaluations of these products using in situ measurements based on the method developed in this study and other methods will be reported in other papers. Suffice to say that many of these gridded products, despite their assimilation of precipitation and other measurements, are still deficient compared with in situ measurements, further demonstrating that the use of gridded precipitation in these data assimilations is not the same as the use of snowfall data in our analysis of the in situ point measurements.

Acknowledgments
This work was supported by NOAA (NA13NES4400003), NASA (NNX14AM02G), and NSF (AGS-0944101). SNOTEL data are obtained from the National Resources Conservation Service (http://www.wcc.nrcs.usda.gov/snow/). COOP data are obtained from the National Center for Atmospheric Research (NCAR) Computational and Informational Systems Lab (CISL) (http://rda.ucar.edu/index.html?hash=cgi-bin/dssearch?words=td3200). PRISM data are obtained from the Oregon State University's PRISM webpage (http://www.prism.oregonstate.edu/). SNODAS data are obtained from the National Snow and Ice Data Center (NSIDC; http://nsidc.org/data/g02158). The authors can be contacted for access to the data generated as part of this study.

References

Bales, R. C., N. P. Molotch, T. H. Painter, M. D. Dettiinger, R. Rice, and J. Dozier (2006), Mountain hydrology of the western United States, *Water Resour. Res.*, *42*, W08432, doi:10.1029/2005WR004387.

Barrett, A. P. (2003), *National Operational Hydrologic Remote Sensing Center Snow Data Assimilation System (SNODAS) Products at NSIDC*, 19 pp., Natl. Snow and Ice Data Cent., Coop. Inst. for Res. in Environ. Sci., Boulder, Colo.

Blanchet, J., C. Marty, and M. Lehning (2009), Extreme value statistics of snowfall in the Swiss Alpine region, *Water Resour. Res.*, *45*, W05424, doi:10.1029/2009WR007916.

Bowling, L. C., D. P. Lettenmaier, B. Nijssen, J. Polcher, R. D. Koster, and D. Lohmann (2003), Simulation of high-latitude hydrological processes in the Torne–Kalix basin: PILPS Phase 2 (e)—3. Equivalent model representation and sensitivity experiments, *Global Planet. Change*, *38*(1), 55–71, doi:10.1016/S0921-8181(03)00005-5.

Brasnett, B. (1999), A global analysis of snow depth for numerical weather prediction, *J. Appl. Meteorol.*, *38*(6), 726–740, doi:10.1175/1520-0450(1999)038<0726:AGAOSD>2.0.CO;2.

Brown, R. D., and B. Brasnett (2010), *Canadian Meteorological Centre (CMC) Daily Snow Depth Analysis Data, Environment Canada*, National Snow and Ice Data Center, Digital Media, Boulder, Colo.

Brown, R. D., B. Brasnett, and D. Robinson (2003), Gridded North American monthly snow depth and snow water equivalent for GCM evaluation, *Atmos. Ocean*, *41*(1), 1–14, doi:10.3137/ao.410101.

Carroll, T., D. Cline, G. Fall, A. Nilsson, L. Li, and A. Rost (2001), NOHRSC operations and the simulation of snow cover properties for the coterminous, *U.S. Proc. Western Snow Conf.*, *69*, 1–14.

Daly, C., R. P. Neilson, and D. L. Phillips (1994), A statistical-topographic model for mapping climatological precipitation over mountainous terrain, *J. Appl. Meteorol.*, *33*(2), 140–158.

Daly, C., M. Halbleib, J. I. Smith, W. P. Gibson, M. K. Doggett, G. H. Taylor, J. Curtis, and P. P. Pasteris (2008), Physiographically sensitive mapping of climatological temperature and precipitation across the conterminous United States, *Int. J. Climatol.*, *28*(15), 2031–2064.

Deems, J. S., S. R. Fassnacht, and K. J. Elder (2008), Interannual consistency in fractal snow depth patterns at two Colorado mountain sites, *J. Hydrometerol.*, *9*(5), 977–988, doi:10.1175/2008JHM901.1.

Drusch, M., D. Vasiljevic, and P. Viterbo (2004), ECMWF's global snow analysis: Assessment and revision based on satellite observations, *J. Appl. Meteorol. Climatol.*, *43*, 1282–1294.

Erxleben, J., K. Elder, and R. Davis (2002), Comparison of aerial interpolation methods for estimating snow distribution in the Colorado Rocky Mountains, *Hydrol. Process.*, *16*(18), 3627–3649, doi:10.1002/hyp.1239.

Fassnacht, S. R., K. A. Dressler, and R. C. Bales (2003), Snow water equivalent interpolation for the Colorado River Basin from snow telemetry (SNOTEL) data, *Water Resour. Res.*, *39*(8), 1208, doi:10.1029/2002WR001512.

Grünewald, T., and M. Lehning (2015), Are flat-field snow depth measurements representative? A comparison of selected index sites with areal snow depth measurements at the small catchment scale, *Hydrol. Process.*, *29*, 1717–1728, doi:10.1002/hyp.10295.

Guan, B., N. P. Molotch, D. E. Waliser, S. M. Jepsen, T. H. Painter, and J. Dozier (2013), Snow water equivalent in the Sierra Nevada: Blending snow sensor observations with snowmelt model simulations, *Water Resour. Res.*, *49*, 5029–5046, doi:10.1002/wrcr.20387.

Helbig, N., A. van Herwijnen, J. Magnusson, and T. Jonas (2015), Fractional snow-covered area parameterization over complex topography, *Hydrol. Earth Syst. Sci.*, *19*, 1339–1351, doi:10.5194/hess-19-1339-2015.

Huntington, T. G., G. A. Hodgkins, B. D. Keim, and R. W. Dudley (2004), Changes in the proportion of precipitation occurring as snow in New England (1949–2000), *J. Clim.*, *17*(13), 2626–2636, doi:10.1175/1520-0442(2004)017<2626:CITPOP>2.0.CO;2.

Knowles, N., M. D. Dettinger, and D. R. Cayan (2006), Trends in snowfall versus rainfall in the western United States, *J. Clim.*, *19*(18), 4545–4559, doi:10.1175/JCLI3850.1.

López-Moreno, J. I., and D. Nogués-Bravo (2006), Interpolating local snow depth data: An evaluation of methods, *Hydrol. Process.*, *20*(10), 2217–2232, doi:10.1002/hyp.6199.

Molotch, N. P., and R. C. Bales (2006), SNOTEL representativeness in the Rio Grande headwaters on the basis of physiographics and remotely sensed snow cover persistence, *Hydrol. Process.*, *20*(4), 723–739, doi:10.1002/hyp.6128.

Niu, G.-Y., and Z.-L. Yang (2007), An observation-based formulation of snow cover fraction and its evaluation over large North American river basins, *J. Geophys. Res.*, *112*, D21101, doi:10.1029/2007JD008674.

Raleigh, M. S., and J. D. Lundquist (2012), Comparing and combining SWE estimates from the SNOW-17 model using PRISM and SWE reconstruction, *Water Resour. Res.*, *48*, W01506, doi:10.1029/2011WR010542.

Reichle, R. H., R. D. Koster, G. J. M. Lannoy, B. A. Forman, Q. Liu, and S. P. P. Mahanama (2011), Assessment and enhancement of MERRA land surface hydrology estimates, *J. Clim.*, *24*, 6322–6338, doi:10.1175/JCLI-D-10-05033.1.

Rienecker, M. M., et al. (2011), MERRA: NASA's Modern-Era Retrospective Analysis for Research and Applications, *J. Clim.*, *24*, 3624–3648.

Rodell, M., et al. (2004), The global land data assimilation system, *Bull. Am. Meteorol. Soc.*, *85*, 381–394.

Saha, S., et al. (2014), The NCEP Climate Forecast System version 2, *J. Clim.*, *27*, 2185–2208, doi:10.1175/JCLI-D-12-00823.1.

Schirmer, M., V. Wirz, A. Clifton, and M. Lehning (2011), Persistence in intra-annual snow depth distribution: 1. Measurements and topographic control, *Water Resour. Res.*, *47*, W09516, doi:10.1029/2010WR009426.

Serreze, M. C., M. P. Clark, R. L. Armstrong, D. A. McGinnis, and R. S. Pulwarty (1999), Characteristics of western United States snowpack from telemetry (SNOTEL) data, *Water Resour. Res.*, *35*, 2145–2160, doi:10.1029/1999WR900090.